Available online at www.sciencedirect.com

ScienceDirect

IFAC Papers Online CONFERENCE PAPER ARCHIVE

IFAC PapersOnLine 56-3 (2023) 253–258

Flocking Control of Multi-agent Automated Vehicles for Curved Driving: A Polyline Leader Approach

Gang Wang and Yan Chen ⋆

Arizona State University, Mesa, AZ 85212 USA (e-mail: gwang109@asu.edu, yanchen@asu.edu)

Abstract: Flocking control for multi-agent automated vehicles has attracted more research interest recently. However, one significant challenge is that the common use of point-shaped virtual leaders giving uniform navigations is unsuitable for vehicle motions with varying relative positions and orientations on multi-lane roads, particularly on curved sections. Considering the practical movements of multi-agent ground vehicles, this paper proposes a novel type of polyline-shaped leader(s) that aligns with multi-lane roads. Specifically, the polyline-shaped leader is composed of line segments that consider road curvatures, different lanes, and the flocking lattice configuration. Moreover, an artificial flow guidance method is applied to provide the direction of velocity references to ensure vehicles move within their respective lanes during the formed flocking. Simulation results demonstrate that the proposed approach can successfully regulate vehicles to drive in their lanes in coordinated motion, which gives fewer structural deviations on curved roads compared to the case with the point-shaped leader.

Keywords: flocking control, multi-agent vehicles, polyline-shaped leader, artificial flow guidance, curved road

1. INTRODUCTION

Flocking control is designed to coordinate a group of agents to achieve a collective behavior (Olfati-Saber (2006)). Due to its potential benefits, including maintaining a constant distance between agents, collision avoidance, and leader tracking, flocking control has gained significant attention in the application of ground vehicles. The exploration of this application has involved investigating the effects of permanent road boundaries (Wang and Chen (2021a)), lane-following in straight roads (Liu and Xu (2015)), non-linear vehicle dynamics (Wang and Chen (2021b)), and heterogenous lattice formation (Wang et al. (2023),Wang et al. (2022)). In this context, flocking agents (automated vehicles) track a reference trajectory through the navigation effect of the virtual leader.

In the literature, the majority of studies on flocking control modeled the (virtual) leader(s), also known as the γ-agent(s), as point mass agents (Wang and Chen (2021a), Su et al. (2009), Su et al. (2008)). The use of the point-shaped leader generates the uniform forces on all α-agents, resulting in a center cluster formation. This phenomenon can be categorized as cluster flocking as documented in (Beaver and Malikopoulos (2021)). However, the importance of the leader's shape in flocking control has not been fully discussed. Moreover, the point-shaped leader is inadequate in considering the orientation and rotational speed on curved roads and generating reference trajectories for path tracking of flocking agents on multiple lanes for multi-agent automated vehicles.

In addition, point-shaped leaders cannot facilitate lane-keeping, which is a crucial aspect of coordinated motion for a group of automated vehicles, particularly on multiple-lane or curved roads. The existing literature on this topic largely focused on the application of flocking control to single-lane roads (Wang and Chen (2021a), Wang et al. (2023)) or lane-free environments (Rostami-Shahrbabaki et al. (2023)), without paying attention to the challenges of lane-keeping on multiple-lane roads. The artificial flow guidance (AFG) method is commonly used in path planning because of its ability to achieve simultaneous good performance in smoothness and completeness, unlike the artificial potential field method (Wang et al. (2017)). Therefore, AFG-based flocking control is a potential method for lane-keeping on multiple-lane or curved roads.

This paper proposes a novel flocking control protocol integrating a polyline-shaped leader with artificial flow guidance (PLL-AFG) to enhance the coordinated motions of automated vehicles. The three main contributions of this paper are summarized as follows.

(1) This paper characterizes the influence of the virtual leader's shape on flocking behaviors for the first time in literature. Three distinct shapes of the virtual leader are defined, namely point, line, and polyline, followed by their interactions with α-agents.
(2) The artificial flow guidance method is utilized to generate the direction of velocity reference for a group of α-agents to move within the corresponding straight

⋆ Corresponding author

This work was supported in part by the Office of Naval Research (ONR) N00014-21-1-2403.

10.1016/j.ifacol.2023.12.033

(or curved) lanes. The control protocol for straight-line driving of the PLL-AFG is obtained by computing the relative position and velocity of α-agents with respect to the reference, which combines the benefits of the AFG's lane-keeping and path planning methods with flocking control using a polyline-shaped leader.

(3) To address conflicts between translational speed consensus of flocking control and varying path lengths of different lanes on curved roads, the control protocol of PLL-AFG is extended to multiple lanes of curved roads. Additionally, the vehicle flocking performance in multiple lanes is measured by defining the structure deviations and off-track errors.

The remainder of this paper is structured as follows. Section 2 defines the point-shaped and line-shaped virtual leaders, together with their influences on group formations. Section 3 proposes the control protocol of PLL-AFG for both straight and curved road scenarios. Section 4 presents the simulation results of PLL-AFG and compares them to those of a point-shaped leader during a straight-to-turn maneuver. Finally, the conclusions are drawn in Section 5.

2. PRELIMINARIES AND (VIRTUAL) LEADERS

This section provides a brief overview of flocking control and artificial flow guidance method. The point-shaped and line-shaped virtual leaders in flocking control are defined, and their potential issues about the applications to coordinated motions of multi-agent vehicles are discussed.

2.1 Flocking Control and Artificial Flow Guidance Method

Flocking Control Considering a group of α-agents (flocking agents) moving on a 2-dimensional plane, we define q_i, p_i, and u_i as the position, velocity, and control input of α-agent i in $\mathbb{R}^m$, respectively, where $i = 1, 2, \cdots, N$. The dynamic motion of the α-agent i is expressed as (1).

$$\begin{cases} \dot{q_i} = p_i \\ \dot{p_i} = u_i \\ u_i = u_i^\alpha + u_i^\beta + u_i^\gamma \end{cases}, i = 1, 2, \cdots, N. \tag{1}$$

The purpose of u_i^α is to establish a flocking lattice, such as a hexagon (Olfati-Saber (2006)) or elliptical lattice (Wang et al. (2023), Wang et al. (2022)), while u_i^β is developed to avoid obstacles. By incorporating the navigation effect of a (virtual) leader, represented by u_i^γ, α-agents can achieve flocking behaviors. This paper concentrates on planar flocking control ($m = 2$) and aims at facilitating the implementation of automated vehicles.

Artificial Flow Guidance An illustration of the artificial flow guidance method (AFG) on a two-lane road is shown in Fig. 1, where A_i is the closest point on the given path to the α-agent, B_i is the preview point based on the preview distance L. The direction of the velocity reference defined in (Gordon et al. (2002)) without normalization is given as follows,

$$v_i = t_{3i}\cos(\theta_i) + \frac{t_{1i} - t_{2i}}{2}, \tag{2}$$

where t_{1i} and t_{2i} are the unit tangent vectors to the reference path r_j at positions A_i and B_i, respectively. t_{3i} is the unit vector from q_i to B_i. θ_i is the half angle between t_{1i} and t_{2i}.

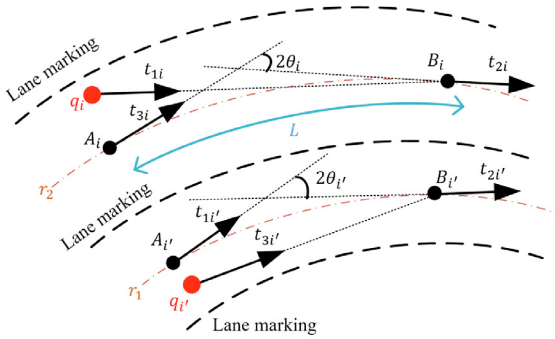

Fig. 1. An illustration of the artificial flow guidance method.

Note that the second term in (2) is a correction factor depending on the reference path (r_j) curvature, and the velocity reference is both normalized and rescaled, as presented in Section 3.

2.2 Point-Shaped and Line-Shaped Leader

The leader, as the group objective, plays a crucial role in achieving collective behaviors of a flock, because of its navigation effect on α-agents. Although different shapes of α-agents, such as point, elliptical, and heterogeneous shapes, were discussed before (Do (2012), Sunkara and Chakravarthy (2017)), how the shape of a (virtual) leader can impact flocking behaviours is not studied yet in the literature.

Many studies utilized point-mass leaders, defined as point-shaped leaders in this paper, to investigate the navigation effects and their impacts on flocking behaviors (Su et al. (2009), Su et al. (2008)). This section aims to define the point-shaped leader and introduce a new line-shaped leader to discuss their impacts on a flocking formation.

Definition 2.1. [Point-shaped leader in flocking control] A point-shaped leader in flocking control is a leader represented by a single moving rendezvous point, described by $q_\gamma \in \mathbb{R}^m$.

Consider a point-shaped leader with the equation of motion (3).

$$\begin{cases} \dot{q_\gamma} = p_\gamma \\ \dot{p_\gamma} = u_\gamma \end{cases} \tag{3}$$

where q_γ, p_γ, and u_γ are the position, velocity, and control input of the point-shaped leader. The navigation effect from a point-shaped leader is defined in (4).

$$u_i^\gamma = c_1^\gamma f(q_\gamma - q_i) + c_2^\gamma g(p_\gamma - p_i), \tag{4}$$

where $f(z) = z$ and $g(z) = z$ are monotonically increasing functions to ensure that the navigation effect is not decreased as z increases in this paper.

Definition 2.2. [Line-shaped leader in flocking control] A line-shaped leader in flocking control is represented by a line l_γ in Euclidean space of $\mathbb{R}^m$. Given a point $\hat{q}_\gamma \in \mathbb{R}^m$ on the line l_γ and the direction vector $\tau_\gamma \in \mathbb{R}^m$ of the line l_γ, any other points on the line $x \in l_\gamma$ satisfy the constraint $(x - \hat{q}_\gamma) \cdot \tau_\gamma = 0$.

The dynamics of the given point on the line-shaped leader are defined in the same manner as that in (3). The

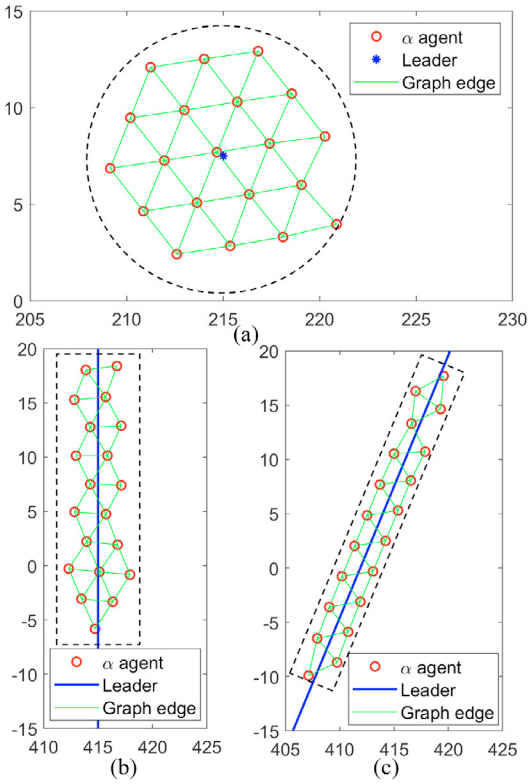

Fig. 2. The impact of leader shapes on flocking lattices: (a) A point-shaped leader leads to a tightly clustered formation; (b) A line-shaped leader at a 90-degree angle results in a rectangular formation; (c) A line-shaped leader at a 67.5-degree angle results in a rectangular formation with the corresponding orientation angle.

navigation effect induced by the line-shaped leader is expressed in (5).

$$u_i^\gamma = c_1^\gamma(\hat{q}_{\gamma i} - q_i) + c_2^\gamma(\hat{p}_{\gamma i} - p_i), \tag{5}$$

where $\hat{q}_{\gamma i}$ and $\hat{p}_{\gamma i}$ are the position and velocity of the point on the line-shaped leader that is closest to α-agent i. $\hat{p}_{\gamma i}$ is obtained by solving the optimization problem in (6).

$$\hat{q}_{\gamma i} = \min_{x \in l_\gamma} ||x - q_i||. \tag{6}$$

where $\|\cdot\|$ is the $2-norm$ operation.

The point-shaped or line-shaped leader applies a navigation force on α-agents, which draws them toward the designated point or line and adjusts their velocities to be consensus of that of the leader. To examine the influence of the leader shape on the formation of a flock, three simulations involving twenty α-agents were conducted to track a virtual leader, in terms of point-shaped, line-shaped at a 90-degree angle, and line-shaped at a 67.5-degree angle, respectively. The final formations of the α-agents are depicted in Fig. 2. A center cluster arrangement of all α-agents is shown in Fig. 2 (a), resulting from the effect of the point-shaped leader. Interestingly, when a line-shaped leader is used, all α-agents converge to a rectangle-like container with the same orientation as the leader, as shown in Fig. 2 (b) and Fig. 2 (c).

For coordinated motions of automated vehicles, the center cluster formation induced by a point-shaped leader may not be sufficient to steer vehicles within their respective lanes without deviation. A line-shaped leader is more suitable for automated vehicles because the orientation and non-center cluster formation are considered. Nonetheless, the flocking lattice may create a potential conflict with such a rectangular formation, as shown in Fig. 2 (b) and Fig. 2 (c). To address this issue, a polyline-shaped leader is proposed next.

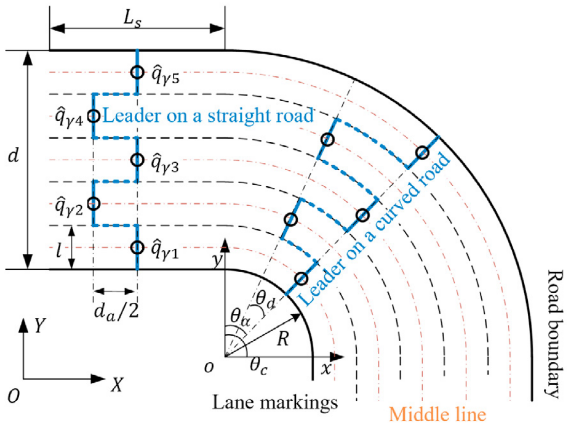

Fig. 3. Five lanes with road boundaries.

3. POLYLINE-SHAPED LEADER OF FLOCKING CONTROL WITH AFG

3.1 Polyline-Shaped Leader in Flocking Control

Definition 3.1. [Polyline-shaped leader in flocking control] A polyline-shaped leader in flocking control with multiple lanes is represented by a series of independent line segments $l_{\gamma j}$ in the Euclidean space of $\mathbb{R}^m$, $j \in \{1, \cdots, M\}$, the line segment $l_{\gamma j}$ corresponds to a specific reference path r_j.

In the context of flocking control, the polyline-shaped leader applies a navigation force on α-agents, and attracts them to the corresponding line segment. Using a polyline-shaped leader for a group of agents can provide corresponding control with respect to the agents' motion in multiple lanes. This is useful in applications where multiple paths are desired, such as automated vehicles in transportation.

The design of a polyline-shaped leader for multi-agent automated vehicles involves several factors that differ from the line-shaped leader, such as the number of lanes, lane width, and most importantly, flocking lattice geometry. To ensure that the center of α-agents on the same lane falls within its corresponding line segment, adjustments must be made for the offset of adjacent line segments, which is influenced by the number of α-agents and flocking lattice geometry. This paper explores this concept further, with a specific focus on the application of PLL-AFG in the elliptical flocking lattice (Wang et al. (2023)) where each lane has the same number of agents. In this case, the offset of adjacent line segments is equal to half the length of the semi-major axis of the ellipse.

3.2 Control Protocol of PLL-AFG in Straight Road

Figure 3 illustrates a polyline-shaped leader in a road with five lanes. In this scenario, the middle line of each

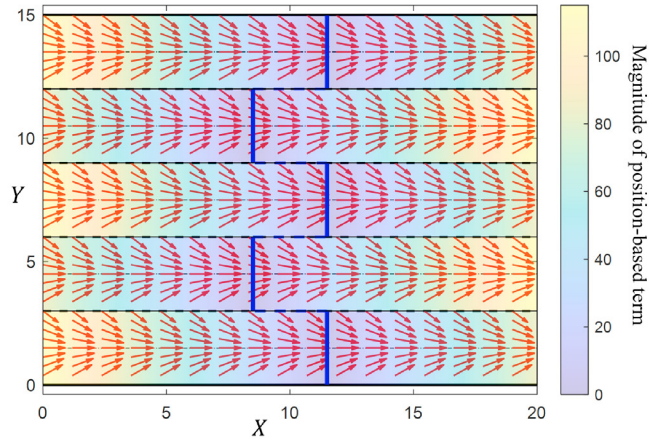

Fig. 4. Navigation effect of a polyline-shaped leader with an artificial flow guidance method on a five-lane road.

lane is chosen as the reference path, with the midpoint of each line segment selected as the position reference. Assuming a fixed point located at the midpoint of the first line segment, with coordinates $\hat{q}_{\gamma 1} = [\hat{q}_{\gamma X1}, \hat{q}_{\gamma Y1}]$ in the global frame XOY, the coordinates of the point $\hat{q}_{\gamma j}$ at the midpoint of line segment j in a straight road can be expressed as follows:

$$\begin{cases} \hat{q}_{\gamma Xj} = \hat{q}_{\gamma X1} - \dfrac{k(j)}{2} d_a \cos(\theta_s) + (j-1) l \sin(\theta_s) \\ \hat{q}_{\gamma Yj} = \hat{q}_{\gamma Y1} - \dfrac{k(j)}{2} d_a \sin(\theta_s) + (j-1) l \cos(\theta_s) \end{cases} \tag{7}$$

where l is the width of the lane, $k(j) = \frac{1+(-1)^j}{2}$, d_a the length of the semi-major axis of the ellipse, θ_s the angle between the tangent direction of the road and the X direction of the global frame.

The velocity reference is defined in (8).

$$v_{\gamma i} = \|p_\gamma\| \frac{v_i}{\|v_i\|}. \tag{8}$$

where v_i is given in (2).

The navigation effect of a polyline-shaped leader on a straight road is defined as follows.

$$u_i^\gamma = \underbrace{c_1^\gamma (\hat{q}_{\gamma i} - A_i)}_{\text{position-based term}} + \underbrace{c_2^\gamma (v_{\gamma i} - p_i)}_{\text{velocity-based term}}. \tag{9}$$

The position-based term is determined by the relative distance between the position reference and its projection point on the path r_i, and the velocity-based term is used to regulate the agent's velocity to the velocity reference in (8).

Fig. 4 shows the navigation effect of a polyline-leader applied to α-agents in (9) on a straight road with five lanes. The red arrow indicates the direction of the velocity reference generated by the AFG, and the face color at each location represents the magnitude of the interaction generated by the position reference. The results illustrate that the navigation effects in (9) are adjusted to accommodate α-agents positioned on different lanes with varying locations.

3.3 Control Protocol of PLL-AFG in Curved Road

Due to the curvature of the road, the computation of position and velocity references becomes more complex compared to a straight road. In this scenario, the polyline-shaped leader maintains a constant angular velocity on each lane. Let xoy be a frame centered at the center of the curve, as depicted in Figure 3, with center coordinates $[o_X, o_Y]$ in the global frame XOY. The angle between adjacent line segments is expressed as,

$$\theta_d = \frac{d_a}{2R + l} \tag{10}$$

Therefore, the expressions for the position reference in frame xoy are obtained,

$$\begin{cases} \hat{q}_{\gamma xj} = S_i [\sin(\theta_\alpha)]^{k(j+1)} [\sin(\theta_\alpha - \theta_d)]^{k(j)} \\ \hat{q}_{\gamma yj} = S_i [\cos(\theta_\alpha)]^{k(j+1)} [\cos(\theta_\alpha - \theta_d)]^{k(j)} \end{cases} \tag{11}$$

where $S_i = R + \frac{2j-1}{2} l$, R is the radius of the curve, and θ_α is derived as,

$$\theta_\alpha = \tan^{-1}\left(\frac{\hat{q}_{\gamma x1}}{\hat{q}_{\gamma y1}}\right) \tag{12}$$

Integrating with the coordinate of o, the position reference in the global frame XOY is expressed as,

$$\begin{cases} \hat{q}_{\gamma Xj} = \hat{q}_{\gamma xj} + o_X \\ \hat{q}_{\gamma Yj} = \hat{q}_{\gamma yj} + o_Y \end{cases} \tag{13}$$

The velocity reference for α-agent i on lane j is defined as,

$$v_{\gamma i} = \|\hat{p}_{\gamma j}\| \frac{v_i}{\|v_i\|}. \tag{14}$$

where $\hat{p}_{\gamma j} = [\hat{p}_{\gamma Xj}, \hat{p}_{\gamma Yj}]$ is given by,

$$\begin{cases} \hat{p}_{\gamma Xj} = \dot{\theta}_\alpha S_i [\cos(\theta_\alpha)]^{k(j+1)} [\cos(\theta_\alpha - \theta_d)]^{k(j)} \\ \hat{p}_{\gamma Yj} = \dot{\theta}_\alpha S_i [-\sin(\theta_\alpha)]^{k(j+1)} [-\sin(\theta_\alpha - \theta_d)]^{k(j)} \end{cases} \tag{15}$$

The navigation effect of PLL-AFG in a curved road is defined as follows.

$$u_i^\gamma = \underbrace{c_1^\gamma t_{1i} \int_{A_i}^{\hat{q}_{\gamma i}} dr_i}_{\text{position-based term}} + \underbrace{c_2^\gamma (v_{\gamma i} - p_i)}_{\text{velocity-based term}}. \tag{16}$$

where r_i is the reference path on the lane i. t_{1i} is given in (2). The position-based term is obtained by measuring the length along r_i between the position reference and A_i (projection point of q_i on r_i). Therefore, this term is applicable not only to curved roads but also to straight roads. The velocity-based term is utilized to alleviate the inconsistency between the velocity consensus in u_i^α and the varying path length on different lanes.

4. SIMULATION RESULTS AND DISCUSSIONS

This section aims to investigate the group dynamics of a flock with an elliptical flocking lattice in straight and curved roads. Specifically, the simulation involves twenty α-agents that track a virtual leader (polyline-shaped or point-shaped leader) on a five-lane road with a straight section followed by a right turn. To evaluate the proposed method's performance, the polyline-shaped leader with artificial flow guidance method (PLL-AFG) and point-shaped leader (PL) flocking control protocols are utilized. Table 1 lists the main simulation parameters. Other simulation parameters, u_i^α and u_i^β, can be found in (Wang et al. (2023)).

Table 1. Parameter values of flocking control

Symbol	Parameter values	Symbol	Parameter values
d_a	5	d_b	$2\sqrt{3}$
L_S	120	R	15
l	3	w	15
c_1^α	10	c_2^α	10
c_1^β	10	c_2^β	10
c_1^γ*	[5,5]	c_2^γ*	[3,10]]

*: [straight section, curved section].

4.1 Simulation Results of PLL-AFG

Fig. 5 shows the position of all α-agents at five different time instants on the straight-to-turn maneuver. The direction of the black arrow shows the α-agent velocity direction, and the length of the black arrow indicates the scaled magnitude of the α-agent velocity. As shown at $t = 0$ s, the initial positions of all α-agents are randomly distributed in a region of $[0, 15] \times [0, 30]$, with zero initial speed. At 2 s, each lane has a nearly equal number of α-agents. The stable formation of the group in the straight road is found at $t = 8$ s, where each lane has four α-agents moving in the middle line, and the elliptical flocking lattice is formed. On the curved road, all α-agents are almost uniformly arranged within their respective lanes, as shown at 12.3 s. After passing the curve, the formation is the same as that on the straight road except for being rotated 90 degrees clockwise as the road direction. In summary, using the PLL-AFG, all agents can automatically become a flock and maintain the elliptical lattice in straight and curved roads, which is in close agreement with our expectations.

Figure 6 displays the speed results of all α-agents in the straight and curved roads in the X and Y directions. The velocity consensus on the straight road is achieved at $t = 6.9$ s in the X direction and $t = 6.7$ s in the Y direction. During the transition from the curve section to the straight section, the velocity in the X direction decreased to 0, while the velocity in the Y direction gradually increased to 8. The velocity consensus is then achieved again at $t = 15$ s in both directions. On the other hand, Figure 7 shows the control inputs for all α-agents in the X and Y directions. The range of control inputs on the curve was much smaller than that on the straight road.

4.2 Comparison Results Between PLL-AFG and PL

Define the structure deviation of a flock as (17).

$$\Gamma = \sum_i \sum_{i \neq j} \left\| q_{ij} - q_{ij}^o \right\| \tag{17}$$

where $q_{ij} = \|q_i - q_j\|$, and q_{ij}^o is the Euclidean distance between α-agent i and α-agent j in the straight road in the stable state. Note that the larger Γ, the larger deviation of the structure is formed.

To quantify the deviation of α-agents to the reference path, the off-track error is selected as the indicator,

$$e_l = \max\{\|q_i - A_i\|\}, i = 1, 2, \cdots, N. \tag{18}$$

During the curved section, the maximum value of Γ and e_l, the minimum inter-agent distance (MID), and the maximum number of agents on the same lane (MNA) are summarized in Table. 2. The findings illustrate that, in comparison to the PL method, the PLL-AFG method

Table 2. Performance of flocking control

Control protocol	Γ_{max}	e_{lmax}	MID	MNA
PL	1144.0	1.5	3.02	6
PLL-AFG	147.9	0.66	3.25	4

demonstrates a reduced degree of structural divergence and maintains a broader safety distance. Additionally, all α-agents are capable of remaining within their respective lanes when transitioning from straight sections to curved sections.

5. CONCLUSION

In this paper, a novel flocking control protocol for multi-agent automated vehicles is presented, which is applicable to both straight and curved driving scenarios. The proposed approach, called PLL-AFG, combines a polyline-shaped leader and an artificial flow guidance method to enable the flocking agents to follow a dedicated path within the lane while in coordinated motion. Simulations of five-lane roads with both straight and curved sections are used to demonstrate the effectiveness of PLL-AFG, and it is compared to a control protocol that uses only a point-shaped leader (PL). The results show that PLL-AFG outperforms PL in terms of structure deviation and off-track errors, as defined in this paper. These findings reveal that PLL-AFG could be beneficial in complex and dynamic transportation environments.

REFERENCES

Beaver, L.E. and Malikopoulos, A.A. (2021). An overview on optimal flocking. *Annual Reviews in Control*, 51, 88–99. doi:https://doi.org/10.1016/j.arcontrol.2021.03.004.

Do, K. (2012). Formation control of multiple elliptical agents with limited sensing ranges. *Automatica*, 48(7), 1330–1338. doi: https://doi.org/10.1016/j.automatica.2012.04.005.

Gordon, T.J., Best, M.C., and Dixon, P.J. (2002). An automated driver based on convergent vector fields. *Proceedings of the Institution of Mechanical Engineers, Part D: Journal of Automobile Engineering*, 216(4), 329–347. doi:10.1243/0954407021529156.

Liu, Y. and Xu, B. (2015). Improved protocols and stability analysis for multivehicle cooperative autonomous systems. *IEEE Transactions on Intelligent Transportation Systems*, 16(5), 2700–2710.

Olfati-Saber, R. (2006). Flocking for multi-agent dynamic systems: algorithms and theory. *IEEE Transactions on automatic control*, 51(3), 401–420.

Rostami-Shahrbabaki, M., Weikl, S., Niels, T., and Bogenberger, K. (2023). Modeling vehicle flocking in lane-free automated traffic. *Transportation Research Record*, 0(0), 03611981231159405. doi: 10.1177/03611981231159405.

Su, H., Wang, X., and Lin, Z. (2009). Flocking of multi-agents with a virtual leader. *IEEE Transactions on Automatic Control*, 54(2), 293–307. doi: 10.1109/TAC.2008.2010897.

Su, H., Wang, X., and Yang, W. (2008). Flocking in multi-agent systems with multiple virtual leaders. *Asian Journal of Control*, 10(2), 238–245. doi: https://doi.org/10.1002/asjc.22.

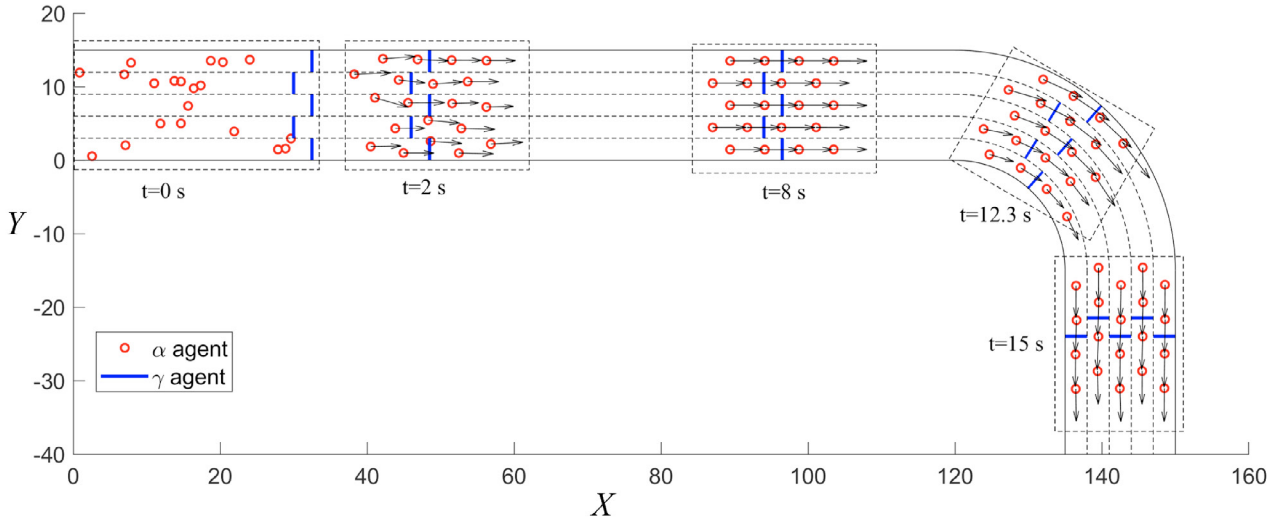

Fig. 5. Formation of all α-agents and the polyline-shaped leader at five different time instants.

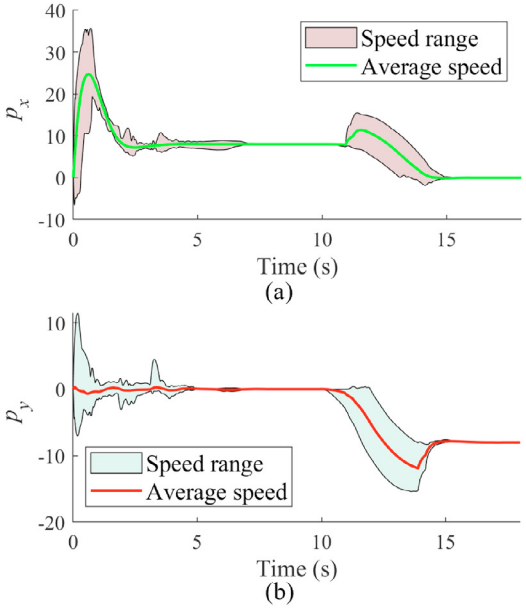

Fig. 6. Speed profiles for all α-agents.

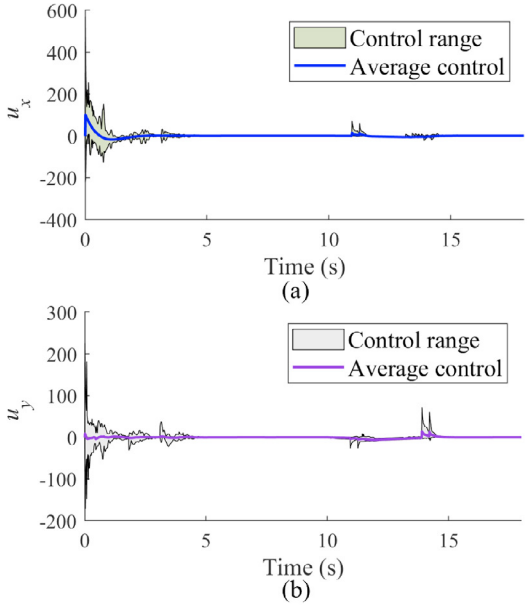

Fig. 7. Flocking control inputs for all α-agents.

Sunkara, V.R. and Chakravarthy, A. (2017). Cooperative collision avoidance and formation control for objects with heterogeneous shapes. *IFAC-PapersOnLine*, 50(1), 10128–10135. doi: https://doi.org/10.1016/j.ifacol.2017.08.1793. 20th IFAC World Congress.

Wang, F. and Chen, Y. (2021a). Flocking control of multi-agent systems with permanent obstacles in strictly confined environments. *Journal of Autonomous Vehicles and Systems*, 1(2). doi:10.1115/1.4052161. 021005.

Wang, F. and Chen, Y. (2021b). A novel hierarchical flocking control framework for connected and automated vehicles. *IEEE Transactions on Intelligent Transportation Systems*, 22(8), 4801–4812. doi: 10.1109/TITS.2020.2986436.

Wang, F., Wang, G., and Chen, Y. (2022). Adaptive spacing policy design of flocking control for multi-agent vehicular systems. *IFAC-PapersOnLine*, 55(37), 524–529. doi:https://doi.org/10.1016/j.ifacol.2022.11.236. 2nd Modeling, Estimation and Control Conference MECC 2022.

Wang, G., Liu, M., Wang, F., and Chen, Y. (2023). A novel and elliptical lattice design of flocking control for multi-agent ground vehicles. *IEEE Control Systems Letters*, 7, 1159–1164. doi:10.1109/LCSYS.2022.3231628.

Wang, N., Song, M., Wang, J., and Gordon, T. (2017). A flow-field guided method of path planning for unmanned ground vehicles. In *2017 IEEE 56th Annual Conference on Decision and Control (CDC)*, 2762–2767. doi: 10.1109/CDC.2017.8264060.